An Investigation of Void Fraction in the Stratified/Annular Flow Regions in Smooth, Horizontal Tubes

D. M. Graham, H. R. Kopke, M. J. Wilson, D. A. Yashar,
J. C. Chato and T. A. Newell

ACRC TR-144 January 1999

For additional information:

Air Conditioning and Refrigeration Center
University of Illinois
Mechanical & Industrial Engineering Dept.
1206 West Green Street
Urbana, IL 61801

(217) 333-3115

Prepared as part of ACRC Project 74
Experimental Investigation of Void Fraction
During Refrigerant Condensation and Evaporation
T. A. Newell and J. C. Chato, Principal Investigators

The Air Conditioning and Refrigeration Center was founded in 1988 with a grant from the estate of Richard W. Kritzer, the founder of Peerless of America Inc. A State of Illinois Technology Challenge Grant helped build the laboratory facilities. The ACRC receives continuing support from the Richard W. Kritzer Endowment and the National Science Foundation. The following organizations have also become sponsors of the Center.

Amana Refrigeration, Inc.
Brazeway, Inc.
Carrier Corporation
Caterpillar, Inc.
Chrysler Corporation
Copeland Corporation
Delphi Harrison Thermal Systems
Eaton Corporation
Frigidaire Company
General Electric Company
Hill PHOENIX
Hussmann Corporation
Hydro Aluminum Adrian, Inc.
Indiana Tube Corporation
Lennox International, Inc.
Modine Manufacturing Co.
Peerless of America, Inc.
The Trane Company
Thermo King Corporation
Visteon Automotive Systems
Whirlpool Corporation
York International, Inc.

For additional information:

Air Conditioning & Refrigeration Center
Mechanical & Industrial Engineering Dept.
University of Illinois
1206 West Green Street
Urbana IL 61801

217 333 3115

An Investigation of Void Fraction in the Stratified/Annular Flow Regions in Smooth, Horizontal Tubes

D. M. Graham, H. R. Kopke, M. J. Wilson, D. A. Yashar, J.C. Chato, and T. A. Newell*
Department of Mechanical and Industrial Engineering
University of Illinois @ Urbana-Champaign
1206 W. Green St.
Urbana, IL 61801
(217-333-1655; t-newell@uiuc.edu)

12/19/98

* Author to whom correspondence should be addressed.

Abstract
Refrigerants R134a and R410A have been used for void fraction measurements in smooth horizontal tubes with diameters between 4mm and 7mm. Quality and mass flux were varied from 5% to 90% and 75 kg/m^2-s to 700 kg/m^2-s, respectively. Two test loops, one for condensing flows at 35C and the other for evaporating flows at 5C, were used in the investigation. Results show that near the transition from annular to stratified flow void fraction changed from viscous-inertial dependence to gravitational-inertial dominated dependence. An important feature observed is the annular flow region's relative insensitivity to mass flux while the border region between annular and stratified flows is characterized by strong mass flux dependence.

Key Words: two-phase flow, annular flow, stratified flow, intermittent flow, horizontal gas-liquid flow, void fraction refrigerants

1. INTRODUCTION

Void fraction is an important parameter for characterizing two-phase flow. This investigation is primarily directed toward flow regimes of interest to the refrigeration industry. In the refrigeration field, the ability to predict void fraction is an important cost consideration. An understanding of the primary factors affecting void fraction in evaporators and condensers can help in the design of "reduced charge" systems. In addition to cost reduction, refrigerant charge minimization is beneficial for environmental and safety reasons.

The ability to predict void fraction can also be used for determining other important flow characteristics such as pressure drop and heat transfer. Among the early works showing the inherent relation between void fraction and pressure drop are the correlation parameters of Lockhart and Martinelli (1949). Traviss, et.al. (1973) used void fraction information in a more basic momentum-energy transfer model for prediction of pressure drop and heat transfer in two-phase condensing refrigerant flow.

Void fraction measurements collected in this study extend results previously available. Two refrigerants, R134a and R410A, representing mid-pressure and high-pressure refrigerants, are used in this investigation. The primary flow regions of interest to refrigeration systems is also an interesting region from a basic viewpoint because it spreads over the annular flow region to the transitional regions for stratified flow and intermittent flow.

Smooth, horizontal tubes with an inside diameter ranging from 4mm to 8mm are the basis for the void fraction measurements. The investigation also examined the effects of heat flux direction (condensation versus evaporation) and heat flux magnitude.

A background section discusses previous work related to void fraction modeling and measurement. An experimental section describes the condenser test loop and evaporator test loop facilities used for the void fraction experiments along with a description of the void fraction measurement technique. Two sections discuss characteristics of the experimental results. One section describes the observed characteristics in terms of mass flux, heat flux, quality, condensation, evaporation, refrigerant, and tube size. The second section examines more basic characteristics of the void fraction results, and discusses potential methods to model void fraction in horizontal tubes for the parameter range investigated.

2. BACKGROUND

A variety of void fraction data has been collected by a number of investigators, and, a wide range of models have been formulated based on these results. Rice (1987) gives a review of many of these models and describes the differences and similarities of their predictions relative to common refrigerants. The comparison reveals the wide level of uncertainty that results when applying void fraction models derived from work based on dissimilar fluids, geometries, and flow conditions.

Many void fraction models may be categorized into two primary groups. One group consists of models that extend the simple homogenous flow model. The second group is characterized by correlations primarily based on the Lockhart-Martinelli parameter that makes use of the relatively unique relation between a two-phase flow and the characteristics of the individual single phase flows. A number of other void fraction models are available that are based on a

variety of parameters. Collier (1980) provides a good description of some of these models and experiments.

Homogenous void fraction models tend to be built from a basic model in which the liquid and vapor phases travel together at a common velocity.

$$\alpha = [1 + ((1-x)/x)(\rho_g/\rho_l)]^{-1} \quad (1)$$

where α = void fraction
x = quality
ρ_g = vapor density
ρ_l = liquid density

Assuming a difference in bulk velocity of each phase, a slip velocity can be introduced.

$$\alpha = [1 + ((1-x)/x)(\rho_g/\rho_l)S]^{-1} \quad (2)$$

where S = slip velocity = vapor velocity/liquid velocity

Various mechanisms have been devised for calculating a slip velocity. Zivi (1964) used a minimization of entropy generation argument and determined that slip ratio is related to the density ratio of the phases. Rigot (1973) made the simple assumption of a constant slip velocity value. Smith (1969) derived a slip velocity model based on the liquid and vapor having the same velocity pressure. Additionally, a tuning factor to account for a fraction of liquid entrained in the core and the remaining liquid fraction separated from the vapor flow was assumed. A model by Ahrens (1987) based on steam/water data from Thom (1964) derived a slip velocity with dependence on phase viscosities and densities. A common feature of all these models is a lack of mass flux dependence.

Lockhart-Martinelli void fraction models are based on the correlation parameter, X_{tt}, which is the square root ratio of the liquid-only pressure gradient to the vapor-only pressure gradient. Models based on the Lockhart-Martinelli parameter are often characterized as ones in which viscous dissipation, such as in the annular flow regime, are dominant. Usually, the "tt" (turbulent liquid-turbulent vapor) form of the X parameter is used. Substituting expressions for single phase, turbulent pressure drop of each pure phase results in a simple expression for X_{tt}.

$$X_{tt} = [(1-x)/x]^{0.9}(\rho_g/\rho_l)^{0.5}(\mu_l/\mu_g)^{0.1} \quad (3)$$

where μ_g = vapor dynamic viscosity
μ_l = liquid dynamic viscosity

Wallis (1969) formulated a void fraction expression based on a simple curvefit with X_{tt} dependence. Domanski (1983) adjusted Wallis's model for X_{tt} values larger than 10. Baroczy (1965) developed a tabular void fraction prediction method based on X_{tt} and a property index related to viscosity and density. Tandon (1985), Premoli (1971), and Hughmark (1962) added additional factors to X_{tt} for void fraction modeling. Tandon's model adds an additional single phase Reynolds number dependence. Premoli added a Weber number dependence as well as a

Reynolds number dependence. Hughmark used a two-phase Reynolds number and a slight Froude number dependence in an implicit void fraction model.

3. EXPERIMENT FACILITIES AND MEASUREMENT TECHNIQUES

3.1 Experiment Facility Descriptions

Two different facilities will be discussed here, one for evaporation tests and the other for condensation experiments. More detailed descriptions of the condenser appear in Graham, et.al.(1998) and Kopke, et.al.(1998), and the evaporator in Wilson, et.al.(1998) and Yashar, et.al.(1998).

Both refrigerant loops are pump driven with mass flow rate adjusted by varying pump speed. Inlet test sections conditions (temperature and quality) are set by using electrical resistance heating strips. The test section heat addition rate in the evaporator is also controlled by electrical resistance heating strips. The condenser uses a counter flow heat exchanger using water to control test section heat transfer. For condenser tests the refrigerant inlet temperature is 35 C while the evaporator refrigerant inlet temperature is 5 C. Inlet quality was varied from almost pure liquid (5%) for evaporation tests, to nearly pure vapor (90%) in condensation tests. The mass flux was varied from 75 kg/m^2-s to 700 kg/m^2-s.

Type T thermocouples are used for temperature measurement and have been found to be accurate within 0.2°C. Pressure transducers located in both loops are accurate to 0.3% of the full scale reading. Electric power measurements use power transducers that are accurate to within 0.2% of their full scale reading. Mass flow measurements use either a Coriolis-type mass flow meter or a positive displacement volumetric flow rate meter.

The test sections are single pass, smooth cylindrical tubes with inside diameters ranging from 4.0 to 8.0 mm. Pressure taps are spaced 1.2 meters apart. Thermocouples are placed at different sites between the pressure taps for test section condition monitoring. Mounting techniques for thermocouples are described in detail by Wattelet(1994) and Dobson(1994). A small diameter tap (approximately 1mm inside diameter) machined from brass is soldered to the test section tube for refrigerant removal. At opposite ends of the test section are shutoff valves with a mechanical linkage connecting the valve handles. The shutoff valves are ball valves with an internal port diameter similar to the test section tube diameter. The linkage allows simultaneous shutoff of the test section for trapping the fluid. A bypass line is opened when the test section is closed in order to keep the loop operating. Detailed descriptions of the each test section and special fittings can be found in Graham, et.al.(1998), Kopke, et.al.(1998), Wilson, et.al. (1998), and Yashar, et.al. (1998).

3.2 Measurement Techniques and Procedures

Void fraction calculations require a known test section volume. While smooth tube volumes can be calculated from the tube geometry, microgrooved tube volume and the volume of special fittings for fluid removal and pressure measurement have volumes that are not easily calculated. A procedure for experimentally determining *in situ* test section volume is used to verify calculated volumes. First, the system is evacuated, and then the test section shutoff valves are closed. Next, a small receiver tank (approximately 1 liter in volume) is filled with either nitrogen, R134a, or R22 gas. The receiving tank is weighed to determine the amount of gas mass in the tank (with +/- 0.01 gram resolution). The tank is then attached to the system via the void

fraction tap, and the gas in the tank is then allowed to enter the test section. Temperature and pressure of the tank and test section are recorded, and the tank is disconnected from the test section. The tank is weighed again to determine how much mass was released into the test section. Using the temperature and pressure of the gas in the test section allows the gas specific volume to be deteremined. The volume of the test section can be found by multiplying by the mass injected into the test section by the specific volume. The three gases used over a range of receiver tank pressures give good agreement in volume. Details and results of the procedure are described by Graham, et.al. (1998).

The void fraction measurement technique is one that has been commonly used by others (Hetsroni(1982)) . To make a void fraction measurement, the shutoff valves on either side of the test section are closed simultaneously, and the bypass line is opened. Pressure transducer lines are closed prior to closing the test section shutoff valves. A valve on the void fraction tap connecting the test section to an evacuated receiver tank is opened, allowing the refrigerant to flow out of the test section and into the tank. The tank is usually cooled and the test section is warmed (on the evaporator) to speed up the process. Once the refrigerant mass has migrated to the receiver tank, the temperature and pressure of the test section are recorded and the void fraction tap valve is closed.

The amount of mass that migrated into the receiving tank is weighed. The vapor mass left in the test section can be determined from the temperature, pressure and volume. The mass in the test section is usually much less than five percent of the mass in the receiver tank. Once the total mass is known, the two-phase specific volume and void fraction of the test section is calculated.

Common sources of error in the experiments are leaks. Refrigerant can leak from loose fittings and improperly soldered joints, resulting in lower than actual amounts of mass in the receiving tank. Also, leaks across the shutoff valves can add refrigerant mass to the receiving tank. Performed properly, this method gives consistent mass readings to within 0.5 gram (usually less than 5%) and void fractions to within 3% at a given condition.

3.3 R134a and R410A Refrigerant Properties

The two refrigerants used for the investigation give a range of properties that are representative of other refrigerants in the mid-pressure to high pressure refrigerant operation range. The table below lists properties of R134a and R410A over the range of conditions investigated. The properties were determined from REFPROP, computer software for refrigerant property determination (NIST (1993)).

Refrg	T	P	Vapor Density	Vapor Viscosity	Liquid Density	Liquid Viscosity
	(C)	(kPa)	(kg/m^3)	(μP)	(kg/m^3)	(μP)
R134a	5	349	16.9	112	1277	2688
R134a	35	888	42.6	128	1165	1884
R410A	5	931	34.4	122	1174	1621
R410A	35	2127	82.5	145	1031	1079

R410A is a "near" azeotropic 50/50 mass mixture of refrigerants R32 and R125. The saturation pressure given in the table is the liquid saturation pressure. The vapor saturation pressure is

approximately 3 to 7 kPa higher than the liquid saturation pressure over the temperature range investigated.

4. EXPERIMENT RESULTS

This section describes void fraction characteristics observed over the range of conditions investigated. The experimental investigation consisted of operating the evaporator and condenser loops over a range of qualities, mass fluxes, and heat fluxes for refrigerants R134a and R410A. Approximately 90 data points for the evaporator and 60 for the condenser were collected. Each data point is the average of two to three void fraction measurements at a given condition. Two tubes with diameters of 4.3 mm and 6.1 mm diameter were used for the evaporator tests. Two tubes with diameters of 6.0 mm and 7.0 mm were used for the condenser tests.

Figures 1 through 4 show void fraction results for the 7 mm diameter tube in condensation and the 6 mm diameter tube in evaporation. Void fraction is plotted as a function of average test section quality. A range of mass flux conditions (75 kg/m^2-s to 450 kg/m^2-s for the condenser and 75 kg/m^2-s to 500 kg/m^2-s for the evaporator) are included on the plots. Figures 1 and 2 show results for the condenser test section using refrigerants R134a and R410A. Figures 3 and 4 show results for the evaporator using R134a and R410A. One of the most important characteristics is the condenser's strong dependence on mass flux at lower mass fluxes. The evaporator data, however, shows relative independence from mass flux. Additional observations indicate R134a's higher void fraction in relation to R410A at similar mass flux and quality conditions. R410A, with a saturation pressure greater than R134a, has a higher vapor density. The smaller evaporator tube (Yashar, et.al. (1998)) also shows mass flux independence over the range of conditions examined (200 to 700 kg/m^2-s), while the smaller condenser tube (Kopke, et.al. (1998)) shows similar mass flux dependence for the lower mass flux range.

The mass flux independence/dependence characteristics of the evaporator and condenser results bring into question the importance of heat flux and heat flow direction. Possibly, liquid deposition and redistribution over the condenser tube's surface makes it more dependent on mass flux than an evaporator where portions of the tube's surface may be prone to dryout.

Figures 5 and 6 illustrate the effect of heat flux and heating direction on void fraction. Figure 5 shows evaporator data from the smaller 4.3 mm tube with R134a over a 0 to 10 kW/m^2 heat flux range. At zero heat flux, inlet and outlet qualities are essentially unchanged (pressure drop is small over the test length and conditions tested). At high heat fluxes and low mass fluxes, the test section quality change is the largest with inlet/outlet quality changes as much as 25%. The average of the inlet and outlet qualities is used as the test section quality in Figure 5. The primary observation from Figure 5 is that heat flux does not seem to significantly affect void fraction. Wattelet's (1994) evaporation heat transfer study indicated that the lower mass flux and quality conditions should have some level of nucleate boiling occurring, however, no effect of this or possible upper tube surface dryout conditions are discernable in the data. A similar plot for the larger evaporator tube also shows void fraction insensitivity to heat flux level (Wilson, et.al. (1998)). Void fraction measurements for large and small tubes in evaporation also showed heat flux insensitivity for refrigerant R410A.

Figure 6 shows data from the condenser loop for the 6 mm tube with R410A. The water-jacket on the flow loop is set up for condensation, and does not offer control of heat flux levels as the electrically heated evaporator loop. In an effort to determine the importance of heat flow direction and magnitude, the water flow to the jacket was closed off in order to achieve a relatively

adiabatic condition. Additionally, the loop was temporarily operated with heated water to the jacket in order to achieve some level of evaporator-like operation. Figure 6 shows the condenser void fraction to remain insensitive to the change of heat flux magnitude and direction. Similar results for R134a were found (Kopke, et.al. (1998)).

Figure 7 illustrates the relative differences between refrigerants R134a and R410A, and the small and large diameter tubes in evaporation. Differences in refrigerant properties resulted in significant void fraction differences, however, no significant differences were observed between the large and small tubes. Similar results are found in condensation (Graham, et.al. (1998) and Kopke, et.al. (1998)), however, the tube diameter difference is less significant than that of the evaporator tests. Dobson's (1994) refrigerant condenser heat transfer results for a 3 mm diameter tube indicate changes in heat transfer that suggests a different type of flow behaviour may occur in smaller tubes. Refrigerant void fraction may also be affected as tube diameters drop below 4 mm.

Overall, the most important observations indicate that refrigerant properties are important. Additionally, possible flow configuration differences may cause lower condenser mass flux conditions to be highly mass flux dependent, while higher condenser mass flux levels and all evaporator conditions tend to have insignificant mass flux dependency. The next section views the void fraction data from a more general viewpoint that explores the flow region characteristics and relative magnitudes of factors that determine flow field configurations.

5. VOID FRACTION DEPENDENCE ON FLOW FIELD CHARACTERISTICS

The previous section illustrates void fraction characteristics in a manner directly related to the refrigerant flows. These results are viewed from a more general perspective in this section in order to examine the physics of the flows and what transitional changes in flow configuration may be occurring.

Flow maps are one way to characterize gas-liquid flows. Generally, the flow configuration is a visual observation. However, other quantified means such as pressure fluctuations (Wattelet (1994)) have also been used to determine the change from one characteristic flow to another. The condenser and evaporator data from this study are plotted together on a Taitel-Dukler (1976) map in Figure 8. Most of the data are in the annular region with low mass flux data being close to the stratified flow region. Data at low vapor qualities tend to be in the intermittent flow region. Figure 9 shows the data plotted in terms of vapor bulk velocity versus liquid bulk velocity. Two points of the data set with liquid velocities significantly higher than corresponding vapor velocities are interesting in that they do not look out of line with other data on the flow region map of Figure 8. Generally, with the exception of those two points, the data shows a slip velocity that ranges in value from 1 to 10.

One might expect the data to be correlated by the Lockhart-Martinelli parameter with most data in the annular flow region where viscous effects tend to dominate dissipation of the flow's energy. A detailed examination of the evaporation and condensation void fraction data (Graham, et.al. (1998), Kopke, et.al. (1998), Wilson, et.al. (1998), and Yashar, et.al. (1998)) indicated that while the evaporation data could be reasonably well modeled by Lockhart-Martinelli and/or slip ratio type models, the condenser data at low mass fluxes could not.

The transition from annular flow to stratified flow is not sharp. A gradual change from annular to stratified flow occurs where the top and side liquid film regions gradually thin. Hurlburt and Newell (1997) have shown that the thickness profile of a liquid film around a tube's perimeter as it transitions between the stratified and annular flow regions can be characterized by a "Froude

rate" type of parameter. Because of the inherent relation between liquid film thickness and void fraction, the parameter should also be relevant for void fraction prediction. The parameter is related to the ratio of the vapor flow's power to the power required to pump liquid from the bottom to top of a tube.

$$\frac{\text{Vapor power}}{\text{Liquid pumping power}} = (0.5*m_v*V_g^2)/ (m_l*g*D) \qquad (4)$$

where D = tube diameter
g = gravitational acceleration
m_l = liquid mass flow rate
m_v = vapor mass flow rate
V_g = vapor velocity

Substituting and rearranging, the power ratio in equation 4 becomes:

$$\frac{\text{Vapor power}}{\text{Liquid pumping power}} = (0.5*G^2*x^3)/ ((1-x)*\rho_g^2*g*D*\alpha^2) \qquad (5)$$

where G = mass flux
x = quality
α = void fraction
ρ_g = vapor density

The Froude rate is the square root of the parameters in equation 5 with the exclusion of void fraction.

$$Ft = \text{Froude rate} = [(G^2*x^3)/ ((1-x)*\rho_g^2*g*D)]^{1/2} \qquad (6)$$

The Froude rate is essentially a Froude number multiplied by the square root ratio of liquid mass flow rate to vapor mass flow rate. In regions where "gravitational drag" becomes dominant, the Froude rate expresses how energy dissipation due to liquid waves and liquid mass movement around the tube's diameter is related to the energy of the flow stream.

Figure 10 is a plot of the void fraction for the evaporation data versus the Froude rate parameter and the Lockhart-Martinelli parameter, X_{tt}. The Lockhart-Martinelli parameter is seen to be a better parameter for correlating the evaporation data. Figure 11 is a plot of the condensation data versus the Froude rate parameter and the Lockhart-Martinelli parameter. The condensation data generally shows better correlation based on the Froude rate parameter. Overall, one would expect a transition from viscous dissipation dominated to gravitational dissipation dominated effects as one moves from annular to stratified flow configurations. A crude but simple way to correlate data that spans this range of effects is a combination of Froude rate and Lockhart-Martinelli parameters. Recognizing that the Lockhart-Martinelli parameter is essentially a ratio of viscous dissipation to inertial energy, the reciprocal Froude rate parameter is needed in order to

express it as a ratio of gravitational energy dissipation to inertial energy. A simple construction for the combined effect on void fraction is assumed as:

$$\alpha = \text{function}(1/Ft + X_{tt})$$

Using a simple curve fit with a form similar to Wallis' (1969) void fraction relation based on X_{tt} only, a simple void fraction correlation is :

$$\alpha = (1 + 1/Ft + X_{tt})^{-0.321} \qquad (7)$$

Figure 12 shows the combined condensation and evaporation data as a function of the combined parameter $(1/Ft + X_{tt})$. Also plotted on Figure 12 is a curve showing the correlation from equation (7). A better correlation may be found by assuming coefficients and exponents for the Ft and Xtt terms. The simple addition of the two drag effects in equation (7) seems to indicate that the two terms have been scaled in a similar manner. Also, the simple superposition of effects may indicate a relative independence between gravitational and viscous effects as the flow field transitions from one region of dominance to the other. Figure 13 is a plot of measured void fraction versus predicted void fraction using equation (7).

6. CONCLUSIONS

Data over a broad range of conditions that bracket common refrigeration evaporation and condensation conditions have been collected. The results generally show that evaporators operate in a range that is dominated by inertial dissipation effects due to the vapor's relatively low density. Condensers, with relatively higher vapor densities, tend to have lower velocities that causes some operational conditions near the transition range to stratified flow. Heat flux magnitude and the direction of heat flux have not been found to significantly effect void fraction. Over the tube diameter range investigated, no significant trends related to tube size have been observed, however, based on results from other researchers, tube diameters 3mm and less should be examined for changes in flow configuration.

A simple correlation based on a combination of viscous and gravitational drag effects has been presented and shown to represent the void fraction better than either viscous or gravitational effects alone. The Froude rate parameter, however, is a crudely formulated dimensional grouping. A more formal development of a Froude rate type of parameter would be useful for more direct understanding of the physics involved in gravity's energy dissipation role.

ACKNOWLEDGEMENTS

The authors express their gratitude to the University of Illinois Air Conditioning and Refrigeration Center, an NSF sponsored/industry supported research center, for financial support of this project.

REFERENCES

Ahrens, F.W. 1983 Heat pump modeling, simulation and design. Proc. of the NATO Advanced Study Inst. on Heat Pump Fund., Espinho, Spain 1980. J. Berghmans, Ed. Martinus Nijhoff Publishers.

Bankoff, S.G. 1960 A variable density single-fluid model for two-phase flow with particular reference to steam-water flow. Transactions ASME, J. of Heat Transfer, **82**, 265-272.

Baroczy, C.J. 1965 Correlation of liquid fraction in two-phase flow with application to liquid metals. Chemical Engineering Progress Symposium Series, **61**, No.57, 179-191.

Collier, J.G. 1980 Convective boiling and condensation. 2nd Ed., McGraw-Hill, 37-54.

Dobson, M.K. 1994 Heat transfer and flow regimes during condensation in horizontal tubes. Ph.D. Thesis, University of Illinois, Urbana, IL.

Domanski, P., Didion, D. 1983 Computer modeling of the vapor compression cycle with constant flow area expansion device. NBS Buidling Science Series 155.

Graham, D.M., Newell, T.A., Chato, J.C. 1998 Experimental investigation of void fraction during refrigerant condensation. ACRC TR-135, Air Conditioning and Refrigeration Center, University of Illinois, Urbana.

Hetsroni, G. 1982 Handbook of multiphase systems, Hemisphere Publishing Corp., 10.24-10.26.

Hurburt, E.T., Newell, T.A. 1997 Modeling of the evaporation and condensation of zeotropic refrigerant mixtures in horizontal, annular flow. ACRC TR-129, Air Conditioning and Refrigeration Center, University of Illinois, Urbana.

Hughmark, G.A. 1962 Holdup in gas-liquid flow. Chemical Engineering Progress, **58**, No.4, 62-65.

Kopke, R.K., Newell, T.A., Chato, J.C. 1998 Experimental investigation of void fraction during refrigerant condensation in horizontal tubes. ACRC TR-142, Air Conditioning and Refrigeration Center, University of Illinois, Urbana.

Levy, S. 1960 Steam slip theoretical prediction from momentum model. Transactions ASME, J. of Heat Transfer, Series C, **82**, 113-124.

Lockhart, R.W. and Martinelli, R.C. 1949 Proposed correlation of data for isothermal two-phase, two-component flow in pipes. Chemical Engineering Progress, **45**, No.1, 39-48.

NIST 1993. NIST thermodynamic properties of refrigerants and refrigerant mixtures. version 4.01. Computer software, National Institute of Science and Technology, Gaithersburg, MD.

Premoli, A., Francesco, D., Prina, A. 1971 A dimensional correlation for evaluating two-phase mixture density. La Termotecnica, **25**, No.1, 17-26.

Rice, C.K. 1987 The effect of void fraction correlation and heat flux assumption on refrigerant charge inventory predictions. ASHRAE Transactions, **93**, Part 1, 341-367.

Sacks, P.S. 1975 Measured characteristics of adiabatic and condensing single component two-phase flow of refrigerant in a 0.377 in. diameter horizontal tube. ASME Winter Annual Meeting, 75-WA/HT-24, Houston, Texas.

Smith, S.L. 1969 Void Fractions in two-phase flow: a correlation based upon an equal velocity head model. Proc. Instn. Mech. Engrs., **184**, Part 1, No. 36, 647-664.

Taitel, Y. and Dukler, A.E. 1976 A model for predicting flow regime transitions in horizontal and near horizontal gas-liquid flow. AIChE Journal, **22**, 45-55.

Tandon, T.N., Varma, H.K., Gupta, C.P. 1985 A void fraction model for annular two-phase flow. Int. J. Heat and Mass Transfer, **28**, No.1, 191-198.

Thom, J.R.S. 1964 Prediction of pressure drop during forced circulation boiling of water. Int. J. Heat and Mass Transfer, **7**, 709-724.

Traviss, D.P., Rohsenow, W.M. and Baron, A.B. 1973 Forced convection condensation inside tubes:a heat transfer equation for condenser design. ASHRAE Transactions, **79**, Part 1, 157-165.

Wallis, G.B. 1969 One-dimensional two-phase flow. McGraw-Hill, 51-54.

Wilson, M.J., Newell, T.A., Chato, J.C. 1998 Experimental investigation of void fraction during horizontal flow in larger diameter refrigeration applications. ACRC TR-140, Air Conditioning and Refrigeration Center, University of Illinois, Urbana.

Wattelet, J.P. 1994 Heat transfer flow regimes of refrigerants in a horizontal-tube evaporator. Ph.D. Thesis, University of Illinois, Urbana, IL.

Yashar, D.A., Newell, T.A., Chato, J.C. 1998 Experimental investigation of void fraction during horizontal flow in smaller diameter refrigeration applications. ACRC TR-141, Air Conditioning and Refrigeration Center, University of Illinois, Urbana.

Zivi, S.M. 1964 Estimation of steady-state steam void-fraction by means of the principle of minimum entropy production. Transactions ASME, J. of Heat Transfer, Series C, **86**, 247-252.

LIST OF FIGURES

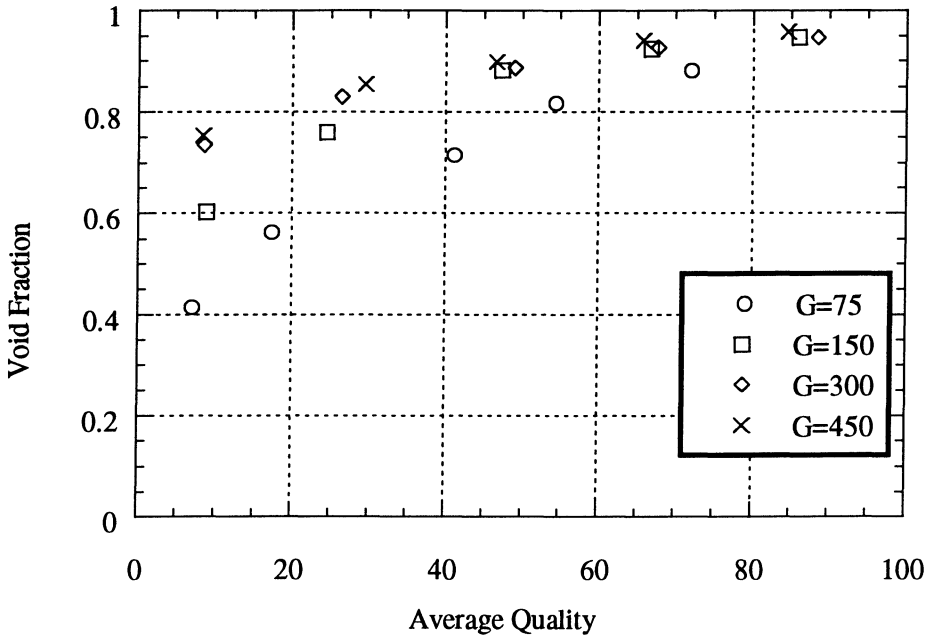

Figure 1 Condenser tube void fraction results for refrigerant R134a in a horizontal, 7.0 mm diameter tube over a range of mass fluxes and qualities.

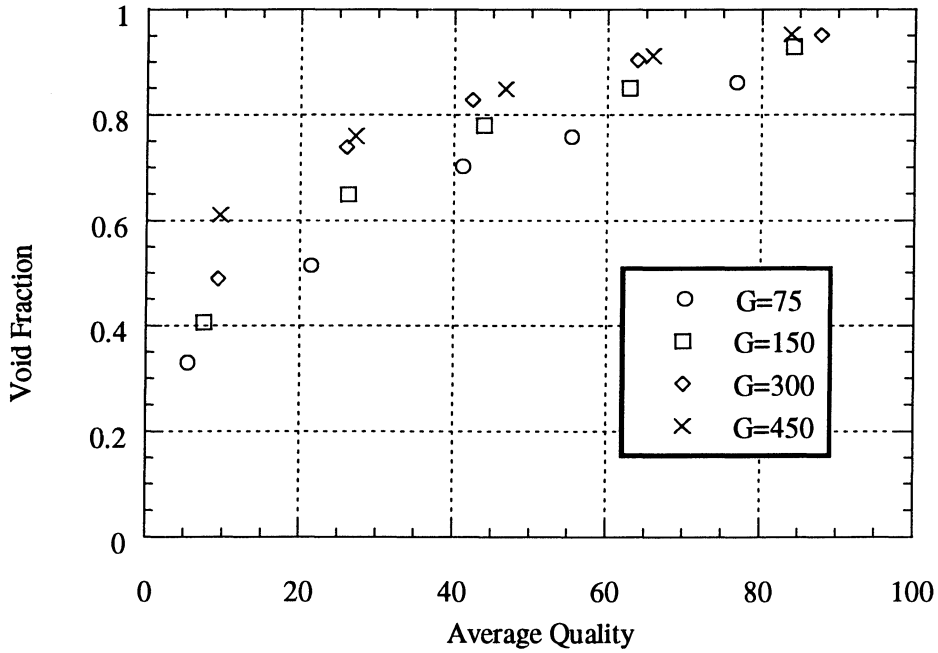

Figure 2 Condenser tube void fraction results for refrigerant R410A in a horizontal, 7.0 mm diameter tube over a range of mass fluxes and qualities.

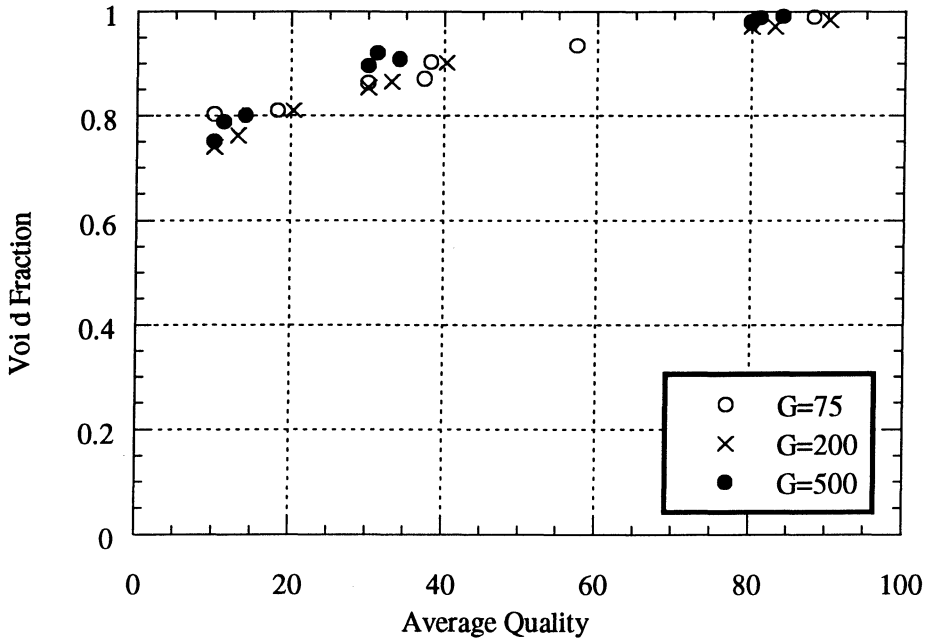

Figure 3 Evaporator tube void fraction results for refrigerant R134a in a horizontal, 6.1 mm diameter tube over a range of mass fluxes and qualities.

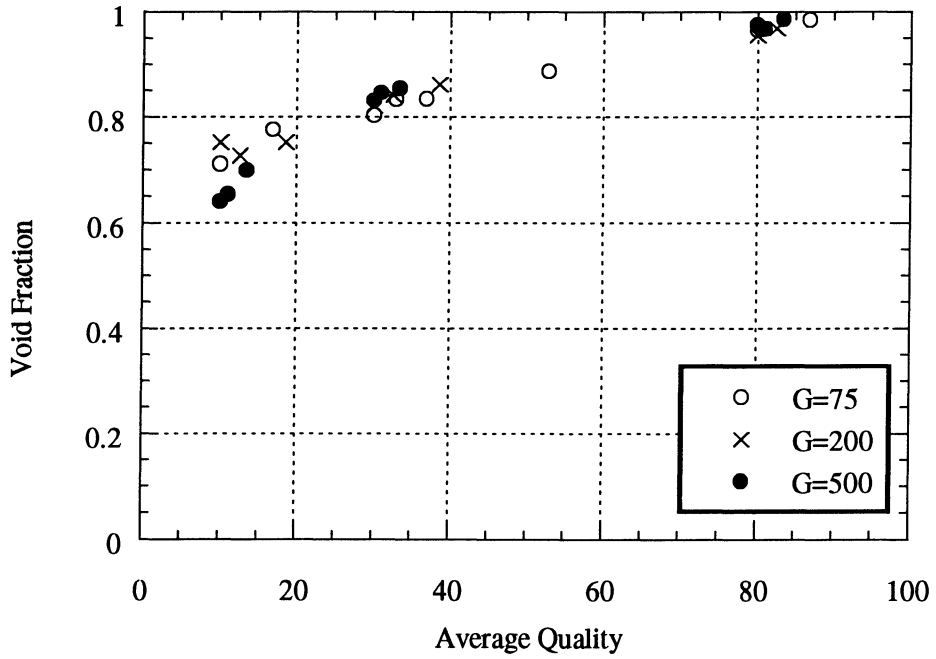

Figure 4 Evaporator tube void fraction results for refrigerant R410A in a horizontal, 6.1 mm diameter tube over a range of mass fluxes and qualities.

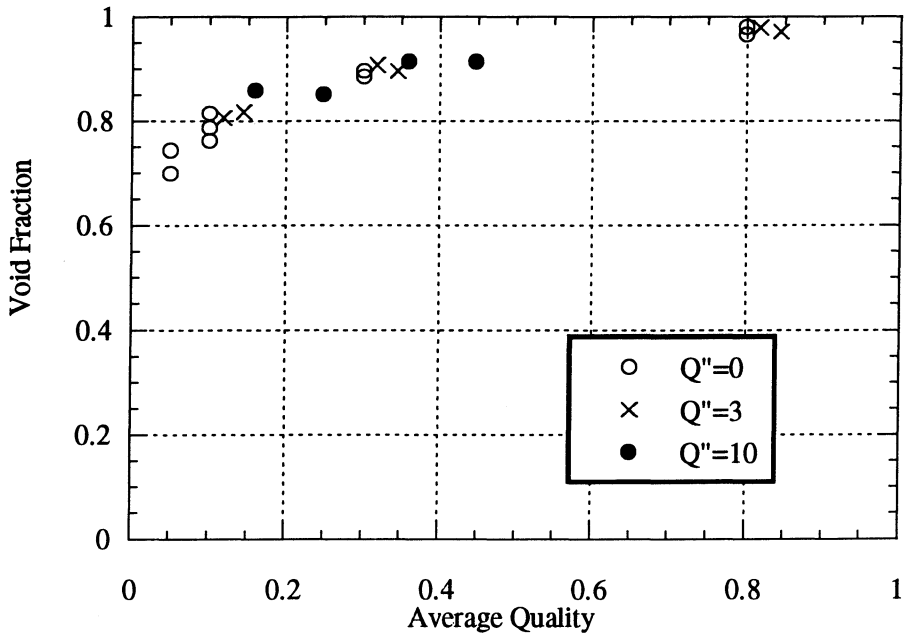

Figure 5 Evaporator tube void fraction results for refrigerant R134a in a horizontal, 4.3 mm diameter tube over a range of qualities and heat fluxes.

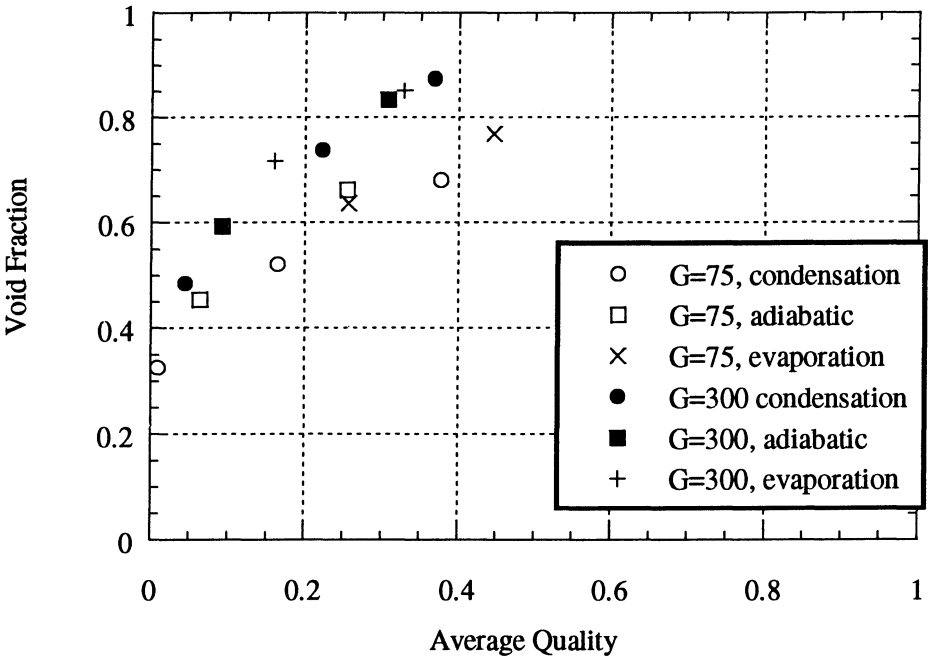

Figure 6 Condenser tube void fraction results for refrigerant R410A in a horizontal, 6.0 mm diameter tube over a range of qualities. Heat flux magnitude and direction (condensation and evaporation) effects are shown.

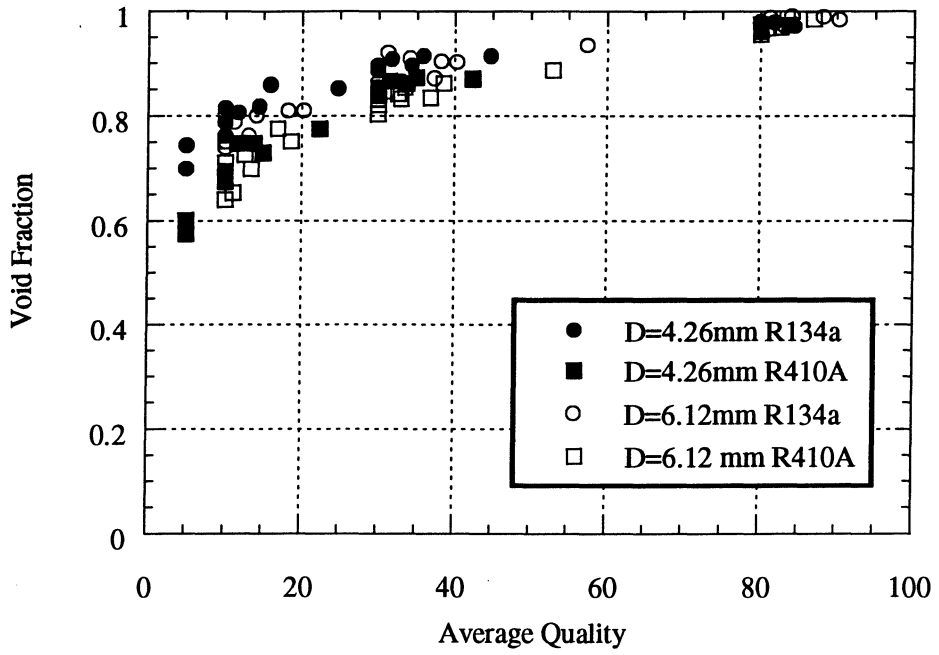

Figure 7 Evaporator tube void fraction results showing effects of tube diameter and refrigerant (R134a and R410A) in a horizontal, 6.1 mm diameter tube.

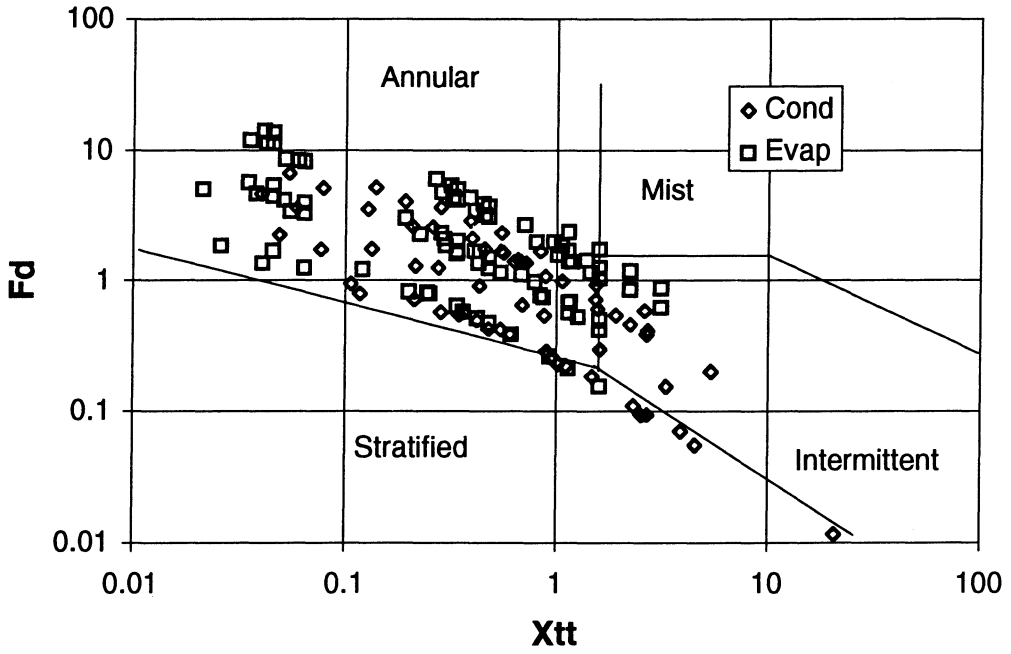

Figure 8 Experimental condenser and evaporator data plotted on a Taitel-Dukler flow map.

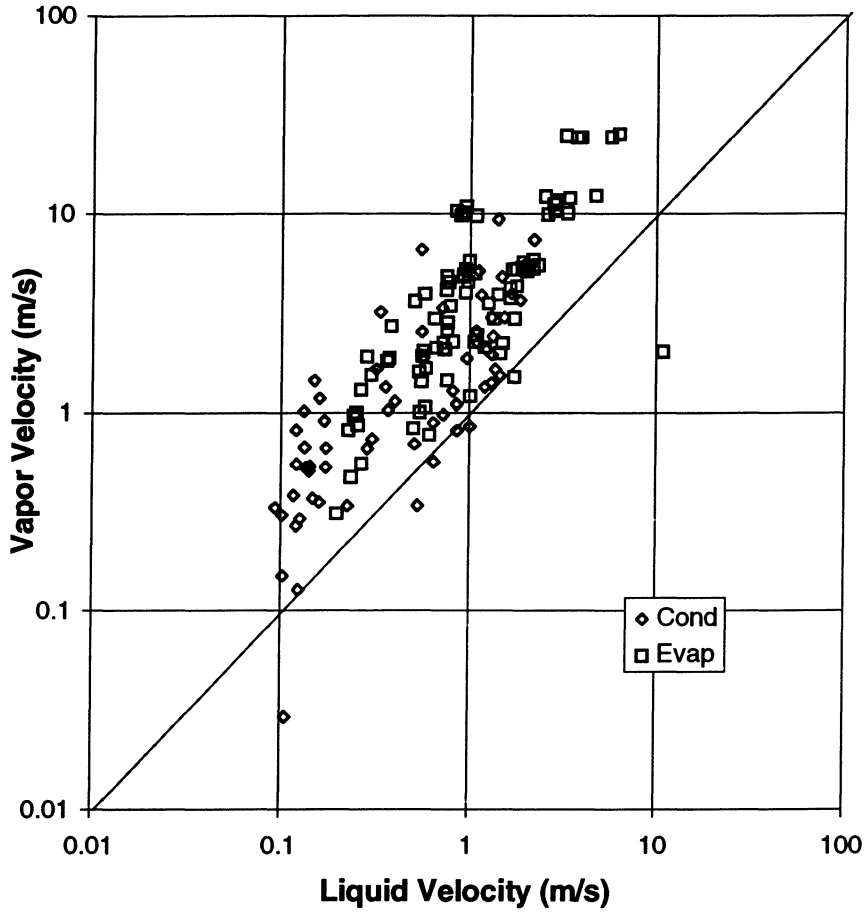

Figure 9 Plot of vapor and liquid velocities for condenser and evaporator data.

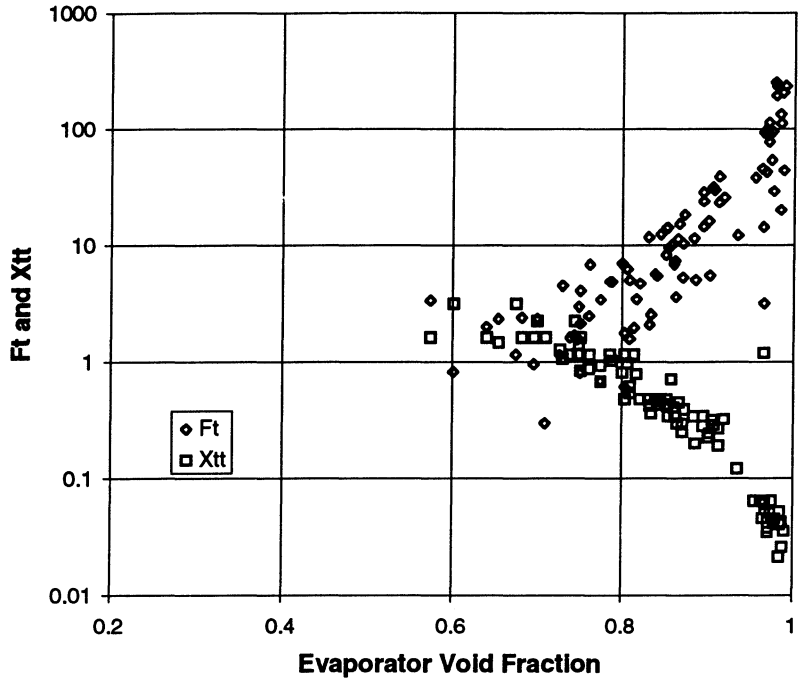

Figure 10 Plot of evaporator data void fraction versus the Froude Rate (Ft) parameter and the Lockhart-Martinelli (Xtt) parameter.

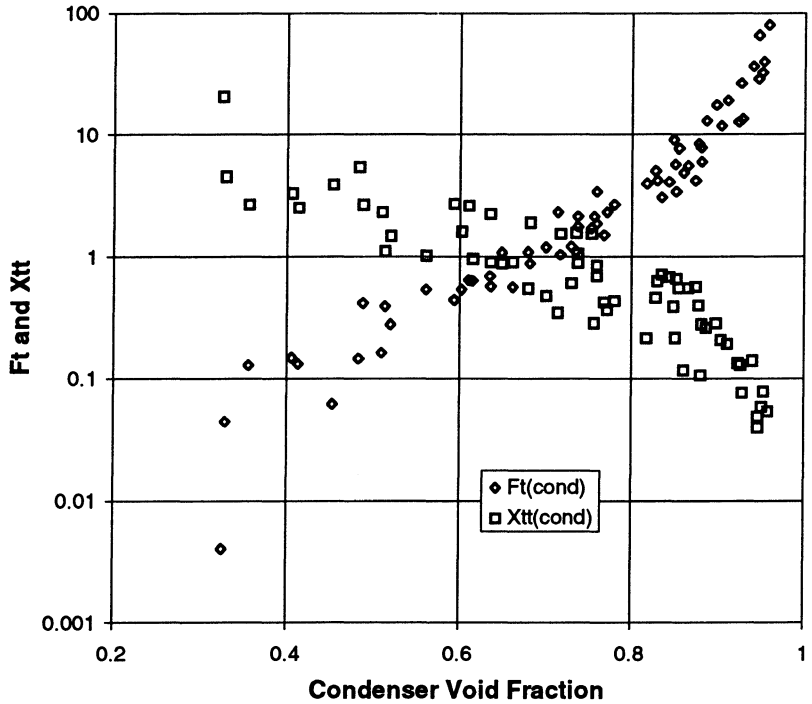

Figure 11 Plot of condenser data void fraction versus the Froude Rate (Ft) parameter and the Lockhart-Martinelli (Xtt) parameter.

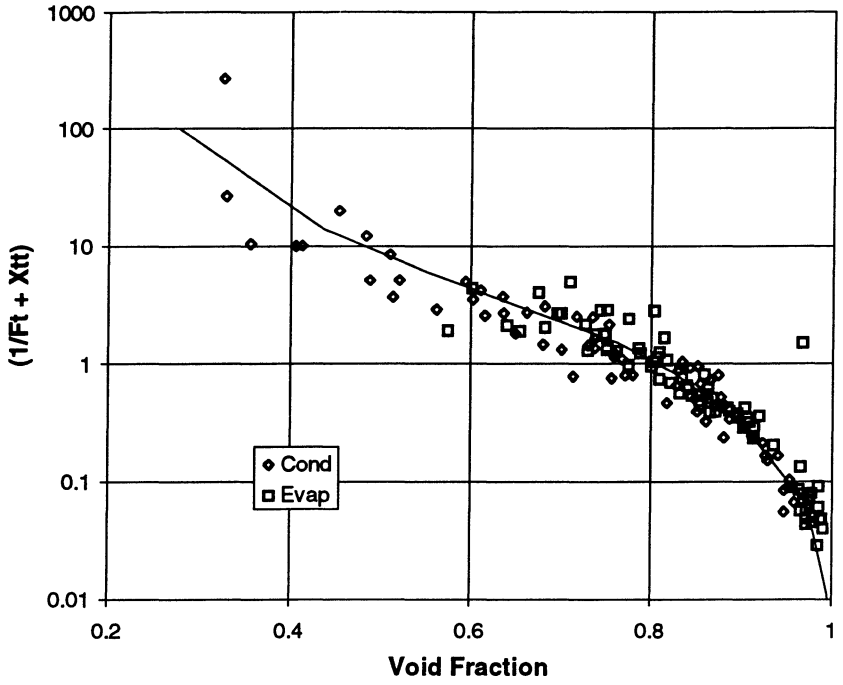

Figure 12 Plot of condenser and evaporator void fraction data versus a combined Froude Rate/ Lockhart -Martinelli parameter.

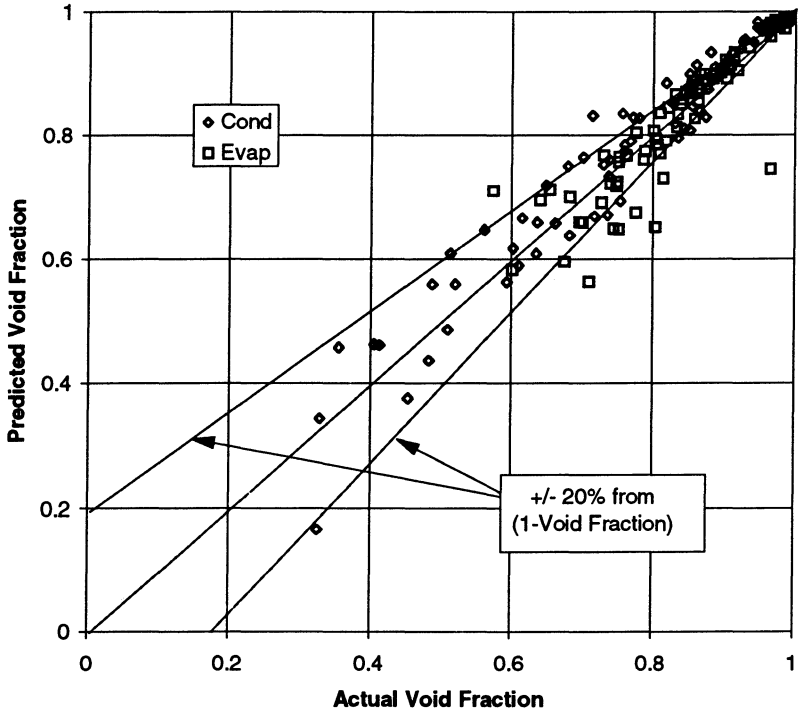

Figure 13 Agreement between actual void fraction data and a simple correlation basied on a combined Froude Rate/Lockhart-Martinelli parameter.